

Coupling A Simple Geometric-Optics Model of Tree Crown Shading with the SAIL Model to Examine Solar Zenith Angle Induced Changes in Forest Reflectance.

Mick Russell, School of Geography and Environmental Studies, University of Tasmania.

Changes in forest crown and understorey shading caused by solar zenith angle variation are examined using a simple geometric-optical forest model. Forests are modelled as randomly spaced eucalypt crowns over a homogeneous understorey. Three forest types representing a gradient of crown density from open dry grassy woodlands to dense wetter closed forest types with an understorey of mesophytic plants are modelled. Fractional coverage of four components: shaded and sunlit canopy and shaded and sunlit understorey are calculated for each forest type. Reflectance of solar radiation in red and near-infrared wavelength bands from each fraction is then modelled for a range of solar zenith angles using the Verhoef SAIL model. The overall scene reflection as seen by a nadir viewing satellite sensor is compared by forest type. Scene reflectance exhibits solar zenith angle induced changes and varies from the reflectance that would be expected from a smooth homogeneous canopy. The extent of the deviation increases with crown density. Modelled changes in scene reflectance are consistent with aircraft measurements carried out at two different solar zenith angles.

INTRODUCTION

Satellite images offer an ideal method of monitoring temporal changes in vegetated surface characteristics at regional scales. However, information extraction systems must be designed to deal with the variability inherent in remote sensing data due to varying solar zenith angle (Z) (Myneni *et al.* 1995). Illumination angles determine the primary path that incident light will trace into the canopy and control the relative proportions of plant tissue that will be illuminated (Pinter *et al.* 1990). Pinter *et al.* (1990) found that over furrowed soil reflectance factors in the red and near infrared were inversely related to Z and could be explained principally by the amount of shadows present; over vegetation, maximum values of reflectance factors in the green and red wavebands occurred at small values of Z and near infrared reflectance factors also varied depending upon Z .

Models of varying complexity have been created to examine the effects of zenith angle on the directional distribution of reflectance (Goel 1988). Many of these models have been developed for homogeneous canopy layers, i.e. the SAIL model (Verhoef 1984). Non homogeneous models often concentrate on row crops for agricultural purposes, (Suits 1985). Notable exceptions to the agricultural models have been the geometric optical models produced by Li, Strahler, Goel and Jupp among others. Using parallel ray geometry and assuming a random array of discrete vegetation crowns, these models estimate the

fraction of a scene that make up the reflectance components.

Components are in effect the sunlit and shadowed proportions of the canopy and understorey surfaces. The vegetation cover is treated as an assemblage of three-dimensional vegetation filled objects that are distinct from one another and are placed on a contrasting background. Each component has a different reflectance characteristic and total surface radiance is determined as a linear sum of the radiance of the individual components (Jupp *et al.* 1986).

In this paper, changes in crown and understorey shading caused by solar zenith angle variation are examined using a simple geometric-optical forest model, the IFC model. Forests are modelled as randomly spaced homogeneous eucalypt crowns over a homogeneous understorey. Fractional coverage of four components: shaded and sunlit canopy and shaded and sunlit understorey are calculated for each forest type. Reflectance of solar radiation in red and near-infrared wavelength bands from each fraction is then modelled for a range of solar zenith angles using the Verhoef SAIL model.

Three vegetation types, representing a gradient from drier to wetter sites, are modelled. They are 1) a relatively open forest with a grassy understorey (wood), 2) a medium density forest with non-touching crowns, and a grassy understorey (dry), and 3) a closed forest with an understorey of mesophytic leaves (wet). Modelled changes due to solar zenith angle are compared to

aircraft measurements carried out over representative forest types.

Vegetation Types

Geometric parameters representative of the vegetation types used in this modelling example are shown in Table 1. The measured data collected from aircraft consist of reflectance in red and near infrared band equivalent to AVHRR channels 1 and 2. Data acquisition, selection, processing, and the vegetation types are similar to those described in more detail in Russell *et al.* (1997)

Parameter	Wood	Dry	Wet
D	4.5	6	8
H	15	15	30
T	5	5	10
R	1.5	0.3	0.0001
Δ	2	2	5
Pt	0.45	0.45	0.6
LA	0.129	0.477	0.806
Tc	0.1	0.1	0.2

Table 1. Parameter values for each vegetation.

THE IFC SHADING MODEL

Areal-proportion models are based around three assumptions (Goel 1988). First, there are only four kinds of scene components visible to a nadir viewing radiometer: sunlit canopy (C_l), shaded canopy (C_s), sunlit background (U_l) and shaded background (U_s). Second, each component is regarded as having a characteristic irradiance I and a characteristic reflectance ρ in each wavelength band λ . Third, the reflectance of the scene is a linear combination of the irradiance of each component modulated by its reflectance value and weighted by its areal proportion (f);

$$\rho_s = f(C_l)\rho(C_l)I(C_l) + f(C_s)\rho(C_s)I(C_s) + f(U_l)\rho(U_l)I(U_l) + f(U_s)\rho(U_s)I(U_s) \quad (1)$$

This formulation requires the determination of three aspects; 1) the areal proportions of the components; 2) the reflectance of each component; and 3) the irradiance incident on each component. Each of these aspects is discussed individually below.

1. Proportions of scene components. f

The method used here is a simplified version of the Jupp *et al.* (1986) multi-layer land cover model. A simple two-layer model is created in which spheroid trees of average dimensions as shown in figure 1 are distributed over a

homogeneous understorey. The tree centres are assumed to have a Poisson distribution. Based on this distribution, geometric-optics is then used to estimate solar zenith angle effects on the amount of shading of both the tree crowns and the background.

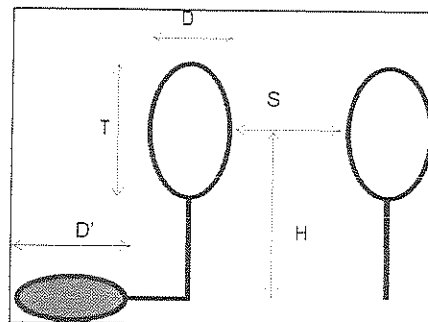


Figure 1. Model dimensions

In the absence of shadows, i.e. at Z equal to zero, the make up of a scene will be determined by the amount of tree canopies as seen from a horizontal projection perspective. This can be calculated as the projection of the crowns onto the horizontal plane. The parameters required to calculate these proportions can easily be obtained from field data collected according to the Walker and Hopkins (1984) field survey method. Crown cover in this survey method is estimated by the (dimensionless) mean gap to diameter ratio (R) defined as the mean distance between crowns divided by the mean crown diameter (S/D as defined in Fig. 1).

The mean horizontal projection of a single crown on the background is determined by;

$$A = \pi D^2 / 4 \quad (2)$$

Walker and Hopkins (1984) determined a relationship between the mean gap ratio and crown density (L) and area as;

$$LA = 0.806 / (1 + R)^2 \quad (3)$$

Where A is in square meters and density is in crowns per square meter.

The expected cover fractions for crowns ($f(C)$) and understorey ($f(U)$) are;

$$f(C) = 1 - e^{-LA} \quad (4)$$

$$f(U) = e^{-LA} \quad (5)$$

At zenith angles other than zero, some fraction between 0 and 1/2 of each crown will be shaded. The mean area of a single sunlit canopy A_C is modelled as 1/2 of A plus an extra fraction, the dimensions of which are determined by Z (Fig. 2).

The fraction of a scene that is made up of lit canopy ($f(C_l)$) and shaded canopy ($f(C_s)$),

respectively are given by;

$$f(C_I) = 1 - e^{-LA_C} \quad (6)$$

$$f(C_S) = f(C) - f(C_I) \quad (7)$$

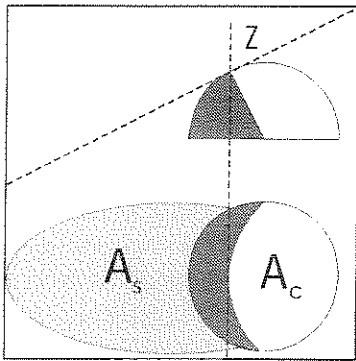


Figure 2. Modelling of crown shading.

At zenith angles other than zero, the amount of understorey that is shaded can be determined by calculating the area of the crowns projected onto the horizontal at an angle equal to the solar zenith angle. Since the crowns are modelled as spheroids with diameter D and depth T , angular projection of the crowns onto the ground will be an ellipse with a normal axis of length D and, after Jupp *et al.* (1985) a second axis of length D' (Figure 1,) dependent on solar zenith angle, where;

$$D' = D(1+b^2) \quad (8)$$

$$b = T / D \tan(Z) \quad (9)$$

Therefore, the mean area of a crown shadow (A'_s) can be found from;

$$A'_s = \pi DD' / 4 \quad (10)$$

For simplicity, the area that is shaded and visible as seen from above (A_s), (Figure 2) is found from;

$$A_s = A'_s - A \quad (11)$$

Using the same distribution as for crowns, the fraction of visible shaded understorey $f(U_S)$ is calculated as;

$$f(U_S) = 1 - e^{-LA_S} \quad (f(U_S) \leq 1 - f(C)) \quad (12)$$

with the maximum value being $1 - f(C)$ (entire visible understorey shaded). And the fraction of the scene made up of unshaded understorey ($f(U_I)$) is calculated as;

$$f(U_I) = 1 - [f(C) - f(U_S)] \quad (13)$$

2. Reflectance of scene components ρ

Reflectance for each component is calculated for red and near infrared bands using the SAIL model (Verhoef 1984). Only nadir reflectance outputs were used. The sources of the vegetative input parameters used are shown in Table 2. The SAIL model also requires a value for the diffuse irradiance, expressed as a fraction of the total irradiance. In the calculation of the reflectance of shaded components, diffuse irradiance was taken as being 1 for both wavelength bands.

For the sunlit canopy, the fractions of diffuse irradiance for clear sky conditions (I_D) were obtained from measurements obtained on the roof of the School of Geography and Environmental studies building.

In the calculation of the SAIL diffuse irradiance parameter for the sunlit understorey (I_D) it was assumed that diffuse irradiance from the sky was reduced by the canopy (represented by LA), and;

$$(I_D) = (1-LA)I_D / [(1-I_D)+(1-LA)I_D] \quad (14)$$

3. Irradiance of Scene Components I

Irradiance incident on sunlit canopy in each band ($I(C_I)$) is taken as 1, with irradiance on other components given as a fraction of sunlit canopy irradiance. Irradiance for shaded canopy, $I(C_S)$ is taken as the measured values I_D .

The irradiance incident on shaded understorey was taken to be: the sum of a term related to the diffuse transmission through the canopy (I_d); plus a term related to side reflection from canopies that are sunlit (I_s); and a trunk reflection term (I_T);

$$I(U_S) = I_d + I_s + I_T \quad (15)$$

Parameter	Component	Source	Comments
LAD (Leaf Angle Distribution)	Crown Understorey -wet -woodland & dry	King (1997) Goel and Streble (1984) Privette <i>et al.</i> (1996)	values for <i>E. macroryncha</i> Planophile Erectophile from grassland
Leaf Transmission τ & reflectance ρ	Crown Understorey -wet woodland & dry	Thomas and Barber (1974) Gates <i>et al.</i> (1965) Walter-Shea <i>et al.</i> (1992)	green leaves of <i>E. urnigera</i> <i>Raphiolepis ovata</i> Average of 3 Prairie grasses.
Soil ρ	All components	Goel (1988)	Sample values from model.

Table 3. For each component, the source used to obtain parameters used in the SAIL model.

I_d is calculated as the sum of the above canopy diffuse irradiance after transmission through canopy gaps and a canopy transmission term;

$$I_d = (1 - P_t) + (P_t * \tau / \Delta) \quad (16)$$

Where P_t refers to the fraction of the canopy that contains foliage when viewed on a horizontal projection. This parameter is equivalent to the canopy type of Walker and Hopkins (1984). τ is the transmissivity of eucalypt leaves and Δ is the leaf area index. I_s & I_T are derived in the Appendix.

The total irradiance incident on sunlit understorey ($I(U)$) is calculated as the above canopy irradiance less the fraction blocked by the canopy plus the side and trunk reflection terms;

$$I(U) = [1 - (I_b(1 - LA))] + I_s + I_T \quad (17)$$

RESULTS

Proportions of Scene Components

Modelled changes in fractional coverage of scene components with zenith angle change are shown in Figure 2. While woodland is dominated by sunlit understorey at all zenith angles, the second most important component changes from sunlit canopy to shaded understorey at zenith angles greater than 65°. In the dry forest, sunlit components dominate the scene at small values of Z . At larger zenith angles the importance of the various scene components changes with an increase in understorey shading. The total proportion of shaded components becomes greater than sunlit components at a zenith angle of 70°. In the wet forest sunlit understorey quickly becomes a minor component and is negligible at a Z of 60°. The transition from sunlit dominance to shade dominance of the scene occurs at a Z of 54°.

Scene Reflectance

Simulated total scene reflectance for the three vegetation types are shown in Figure 3. The model indicates a decrease in visible reflectance as the solar zenith angle increases. This decrease occurs at the greatest rate for the dry forest. The woodland visible reflectance is midway between the reflectance modelled for a homogeneous pasture (past) and that expected from a eucalypt dominated dry forest. At very large solar zenith angles the model indicates that reflectance is similar for both wet and dry forests. At these Z 's, much of the scene reflectance is dominated by a sunlit canopy of eucalypt crowns with an effectively large leaf area index due to the low solar angle. At small solar zenith angles, wet

forest reflectance will have a greater contribution from the less reflective understorey.

The modelled near infrared reflectance for the two forest types shows considerable deviation from the SAIL output for homogeneous pasture or eucalypt canopy (euc). SAIL indicates an increase in reflectance for homogeneous canopies as solar zenith angle increases for angles up to 70°. IFC produces a similar trend for woodland. However, for both forest types, IFC indicates a decrease in infrared reflection as solar zenith angle increases. Figure 4 shows the measured reflectance from the three forest types and from pasture collected from aircraft. The data show similar trends to those simulated by the model.

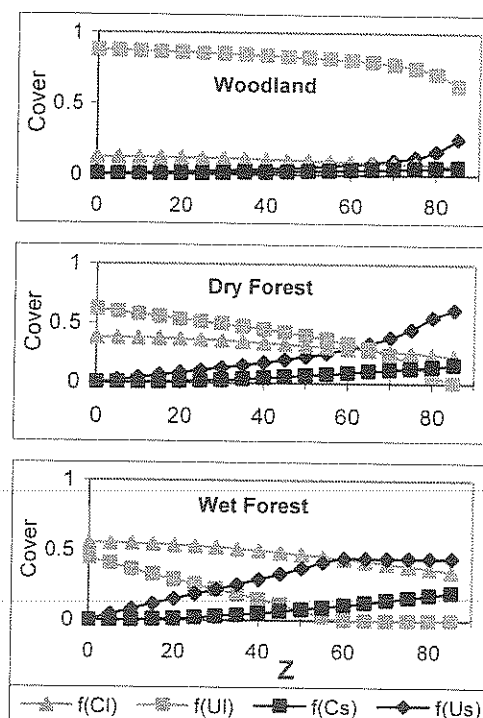


Figure 2. Fractional coverage of scene components of the three forest types.

DISCUSSION

The aim of the model simulations presented was to examine trends in reflectance changes due to solar zenith angle variations and to compare these trends with reflectance changes modelled using a homogeneous canopy. Because of the vertical orientation of eucalypt leaves in forest canopies, an increase in solar zenith angle leads to a greater effective LAI due to the longer path-length through the canopy. Models based on a homogeneous canopy simulate a decrease in reflectance in visible wavelengths and an increase in the near infrared with larger solar zenith angles. The IFC model takes into account changes in the proportion of sunlit and shaded components with solar zenith angle changes. For

the forests, increases in solar zenith angle results in increased contributions from shaded components which have a lower irradiance, hence the scene reflectance is lower.

Comparison of modelled and measured visible reflectance indicates that the model captures the relatively more rapid decline in reflectance from the dry forest canopy as solar zenith angle increases. Given that the parameters used in the model are based on either typical or previously published values the model performs well in estimating reflectance from the different vegetation types.

In the near infrared, modelled reflectances are much higher than measured values. This could be expected given the method of choosing SAIL parameters for soil, grass and eucalypt leaf reflectance values. Increased shading at large solar zenith angles is more pronounced in the near infrared due to rapid light attrition as a result of the high leaf reflectivity at these wavelengths. For the forests, this leads to greater contributions from shaded components to the

overall scene reflectance at larger solar zenith angles, resulting in a decrease in scene reflectance. Due to the more homogeneous nature of the woodland, shading effects only occur at very large solar zenith angles.

CONCLUSION

A decrease in the proportions of sunlit surfaces due to tree crown shading within forest canopies leads to a decrease in total scene reflectance as solar zenith angle increases. This decrease occurs for both red and near infrared wavelengths. These effects are not accounted for by the processes of individual leaf shading used in models devised for randomly distributed leaves in a homogeneous canopy. Deviation from homogeneous models is more pronounced in the near infrared band.

The IFC model offers a step towards an improvement over models of homogeneous canopies in the temporal correction of satellite images taken at different solar zenith angles.

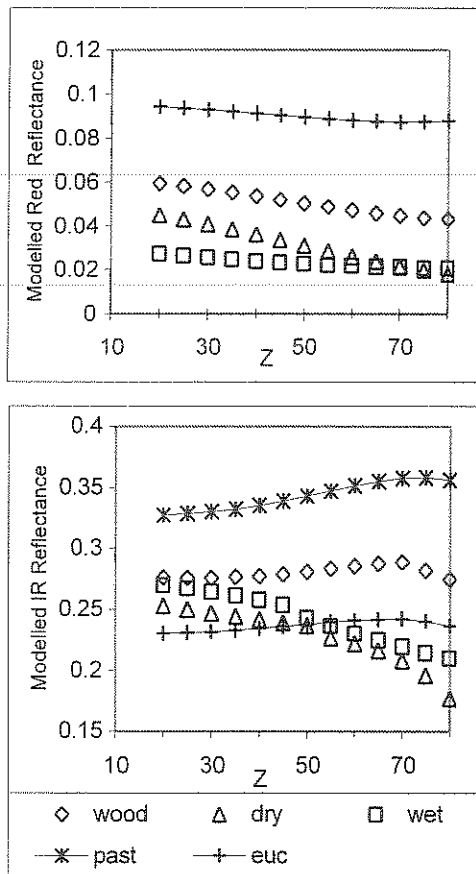


Figure 3. Modelled reflectance.

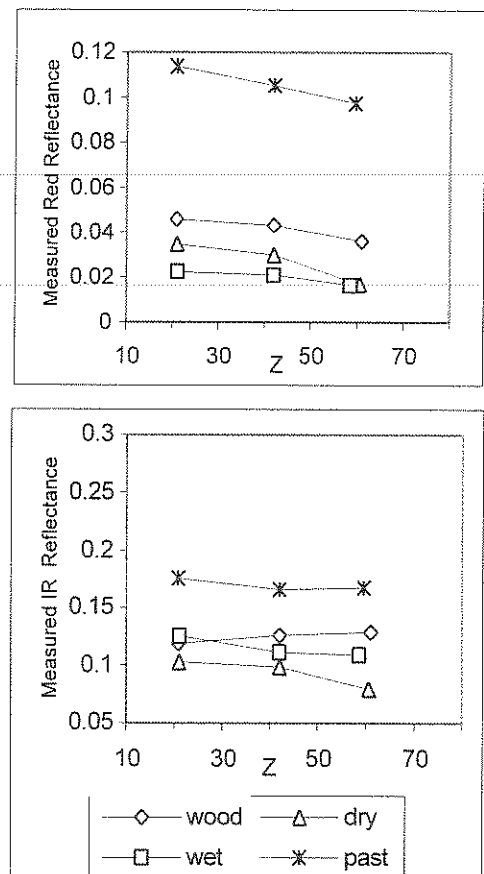


Figure 4. Measured reflectance.

REFERENCES

- Gates, D.M., Keegan, H.J., Schleter, J.C. and Weidner, V.R., Spectral properties of plants, *Appl. Opt.*, 4, 11-20, 1965.
- Goel, N.S. and Streble, D.E., Simple beta distribution representation of leaf orientation in vegetation canopies, *Agron. J.*, 76, 800-803, 1984.
- Goel, N.S., Models of vegetation canopy reflectance and their use in estimation of biophysical parameters from reflectance data, *Remote Sensing Reviews*, 4, 1-212, 1988.
- Jupp, D.L.B., Walker, J. and Penridge, L.K., Interpretation of vegetation structure in Landsat MSS imagery: A case study in disturbed semi-arid eucalypt woodland. Part 2. Model-based analysis, *J. Environmental Manag.*, 23, 35-57, 1986.
- King, D.A., The functional significance of leaf angle in Eucalyptus, *Aust. J. Bot.*, 619-639, 1997.
- Myneni, R.B., Maggion, S., Jaquinta, J., Privette, J.L., Gobron, N., Pinty, B., Kimes, D.S., Verstraete, M.M. and Williams, D.L., Optical Remote Sensing of vegetation: Modeling, caveats, and algorithms, *Remote Sens. Environ.*, 52, 169-188, 1995.
- Pinter, P.J., Jackson, R.D. and Moran, M.S., Bidirectional reflectance factors of agricultural targets: A comparison of ground-, aircraft-, and satellite-based observations, *Remote Sens. Environ.*, 32, 215-228, 1990.
- Privette, J.L., Emery, W.J. and Schimel, D.S., Inversion of a vegetation reflectance model with NOAA AVHRR data, *Remote Sens. Environ.*, 58, 187-200, 1996.
- Russell, M.J., Nunez, M., Chladil, M.A., Valiente, J.A. and Lopez-Baeza, E., Conversion of nadir, narrowband reflectance in red and near-infrared channels to hemispherical surface albedo, *Remote Sens. Environ.*, 61, 16-23, 1997.
- Suits, G.H., An analysis of spectral discrimination between corn and soybean using a row crop reflectance model, *Remote Sens. Environ.*, 17, 109-116, 1985.
- Thomas, D.A. and Barber, H.N., Studies on leaf characteristics of a cline of Eucalyptus urnigera from Mount Wellington, Tasmania, II: Reflection, transmission and absorption of radiation, *Aust. J. Bot.*, 22 701-707, 1974.
- Verhoef, W., Light scattering by leaf layers with application to canopy reflectance modeling: The SAIL model, *Remote Sens. Environ.*, 16, 125-141, 1984.
- Walker, J. and Hopkins, M.S., Vegetation In Australian Soil and Land Survey Handbook (McDonald, R.C., Isbell, R.F., Speight, J.G. Walker, J. and Hopkins, M.S. eds), Inkata Press, Melbourne, 46-67, 1984.
- Walter-Shea, E.A., Blad, B.L., Hays, C.J., Mesarch, M.A., Deering, D.W. and Middleton, E.M., Biophysical properties affecting vegetative canopy reflectance and adsorbed photosynthetically active radiation at the FIFE site, *J. Geophys. Res.*, 97, 18925-18934, 1992.

Appendix.

Calculation of the fraction of radiation scattered from the side of a sunlit crown (I_s). Both the fraction of the side of the crown that is sunlit (P_l) and the angle of incidence of the radiance on the leaves are solar zenith angle dependent. (I_s) was calculated for each solar zenith angle.

(1) It was assumed that at least 1/2 of one side of a crown was sunlit.

(2) The extra fraction of the side of a crown that was sunlit was estimated geometrically.

(3) The SAIL model was run using an inverted eucalypt LAD and an input solar zenith angle equal to 90-Z (i.e. simulating the vertical canopy). SAIL was configured to output reflectance values for view azimuth angles 90° - 270° (i.e. towards the ground) in 10° steps and for view zenith angles 55° - 85° in 10° steps (i.e. away from the crown, with 90° representing an area directly below the edge of a crown and lower values representing areas further away).

(4) A view azimuthally averaged reflectance I_n was calculated where n is one of 5 view angle groups; 90-85, 90-80, 90-75, 90-70, and 90-60.

(5) The relevant group used in the calculation of I_s for each vegetation type is dependent on the proportion of visible understorey and was determined by the parameter Ω ;

$$\Omega = \text{atan}(H / W + D/2) \quad (18)$$

Half of the visible canopy was assumed to be sunlit and scattered irradiance was calculated as;

$$I_s = 1/2 * LA * P_l * I_n \quad (19)$$

Reflection from trunks (I_T) was calculated as;

$$[1/2 * T_c * \rho_T] \quad (20)$$

Where T_c is the fraction of trunk visible and ρ_T is the average reflectance from trunks based on measured values.